SEMARAK ILMU PUBLISHING

Semarak Engineering Journal

Journal homepage:
https://semarakilmu.com/
ISSN: 3036-0145



Chemical Reaction and Stefan blowing analysis of Eyring- Powell nanofluid over a stretched surface with Thermal Radiation

M. Gnaneswara Reddy[1], S. Kiranmaiye[1], Kalyan Kumar Challa[2], M. Eswara Rao[3,*], Muhammad Jawad[4]

[1] Department of Mathematics, Acharya Nagarjuna University Campus, Ongole 523 001, Andhra Pradesh, India
[2] Department of Mathematics, Narayana Engineering College (Autonomous), Gudur, Tirupati-524 101, India
[3] Department of Mathematics, Saveetha School of Engineering, SIMATS, Chennai, Tamil Nadu
[4] Department of Mathematics, The University of Faisalabad, Faisalabad, 38000, Pakistan

ARTICLE INFO

Article history:
Received 24 March 2025
Received in revised form 6 May 2025
Accepted 6 July 2025
Available online 6 October 2025

Keywords:
MHD; Chemical reaction; Stefan blowing; Powell - Eyring nanofluid; thermal radiation

ABSTRACT

This paper presents a comprehensive study on the magnetohydrodynamic flow of an Eyring-Powell nanofluid over a stretchable surface, focusing on the significant effects of chemical reactions, Stefan blowing, and thermal radiation. The research employs advanced numerical techniques and similarity transformations to convert critical partial differential equations governing momentum, concentration, and temperature into a manageable system of non-linear ordinary differential equations. The outcomes of critical physical parameters are acquired by engaging the built-in bvp4c solver in the MATLAB computational software. The computational approach utilized in this study is validated through a comparison with existing literature, showcasing a high degree of agreement with previous results. This reinforces the reliability of the numerical methods employed and the relevance of the findings. The profiles of velocity, temperature, and concentration as well as the related physiological traits that are used in the study have been identified. The intricate relationship between the skin friction coefficient, Sherwood number, and Nusselt number, and their impact on mass and heat transfer characteristics, has been a subject of extensive research in various fields, including fluid dynamics, heat transfer, and chemical engineering. Key results indicate that an increase in the thermal radiation parameter leads to a notable rise in temperature distribution, enhancing heat transfer rates. Specifically, the study finds that the temperature increases significantly with higher thermophoresis and Brownian motion parameters, which facilitate better thermal energy transfer. Additionally, the concentration field shows a substantial decrease with an increased chemical reaction rate, highlighting the impact of reaction kinetics on mass transfer.The study reveals that the inclusion of Stefan blowing significantly influences fluid motion, leading to increased velocity profiles due to the introduction of additional momentum into the boundary layer. This effect is crucial for applications requiring efficient fluid transport.

* *Corresponding author.*
E-mail address: mannerieswar99@gmail.com

1. Introduction

The study of fluid flow over a stretching surface has been a topic of significant interest in the field of fluid dynamics, particularly due to its numerous applications in various industries, such as polymer processing, metal extrusion, and chemical engineering [1-5]. Haider *et al.,* [6] examined the unsteady MHD nanofluid flow past a stretching surface when Stefan blowing or suction was present. Abbas and Megahed [7] studied the impact of chemical reaction on hydromagnetic non-Newtonian fluid flow because of a slendering stretching sheet. They proposed a mathematical model and derived similarity solutions for the governing equations. In the presence of Stefan blowing or suction, Konai *et al.,* [8] embarked the Casson nanofluid flow past a stretching surface. The analytical analysis conducted by Sankari *et al.,* [9] on the double stratification of Casson nanofluid over an exponential stretching surface demonstrates a comprehensive exploration, specifically delving into the characteristics of non-Newtonian fluids and the behavior of nanofluids. Zeb *et al.,* [10] investigated the impacts of both magnetic dipole and Arrhenius activation energy on the ferrofluid flow across a stretching surface. Ali *et al.,* [11] investigated the combined effects of radiation, activation energy, and an electro-periodic magneto-hydrodynamics on the non-linear flow across a stretching sheet. Zhang *et al.,* [12] explored the effects of Stefan's blowing and thermal radiation on Jeffery nanofluid flow over a stretching sheet.

The Powell-Eyring fluid model, a widely employed rheological framework, captures the intricate dynamics of non-Newtonian fluids. The findings indicate that the fluid time scale is extremely sensitive to small variations in the zero-shear rate viscosity, while it exhibits moderate sensitivity to changes in the infinite shear rate viscosity. The ability to accurately predict the rheological behavior of fluids is crucial in numerous industrial and engineering applications, ranging from polymer processing to oil and gas extraction. By understanding the sensitivity of the model parameters, researchers can better assess the robustness and applicability of the Powell-Eyring fluid model in diverse scenarios [13-18]. Alsaedi *et al.,* [19] investigated the impacts of both Joule heating and nonlinear mixed convection on the Powell- Eyring nanofluid flow across a stretching surface. Aljabali et al*.,* [20] provided a comprehensive analysis of the steady two-dimensional flow of a Powell-Eyring fluid across a shrinking sheet. Allehiany *et al.,* [21] investigated the impacts of both magnetic and natural convection on Cilia flow of Powell-Eyring nanofluid in a channel. In a slippery boundary wall, Akinola *et al.,* [22] embarked the intricate interactions between electromagnetic viscous heating, thermal radiation, and temperature propagation of Powell- Eyring fluid. Ullah *et al.,* [23] studied the steady, fluctuating, turbulence, amplitude and oscillatory behavior of skin friction, heat flux and mass flux along vertical heat exchanger plate. Recently, Challa *et al.,* [24] examined the flow characteristics of Powell- Eyring nanofluid passing over an unsteady stretching surface subject to Stefan blowing/suction.

The study of complex fluid flow and heat transfer processes has become increasingly important in various engineering and industrial applications, given their critical role in optimizing system performance, enhancing efficiency, and ensuring safety. One such area of interest is the investigation of magnetohydrodynamic radiative heat transfer in non-Newtonian Eyring–Powell fluid models [25-28]. Daniel and Daniel [29] explored the effects of buoyancy and thermal radiation on Magnetohydrodynamic (MHD) flow over a stretching porous sheet using the homotopy analysis method. This exploration delved into the subtle nuances of how buoyancy and thermal radiation influence the intricate dynamics of MHD flow over-stretching porous surfaces undergoing stretching. Chamkha *et al.,* [30] delved into a detailed exploration of the combined influences of thermal radiation and buoyancy on a hydromagnetic drift over an accelerating permeable surface, considering the existence of a heat source or sink. This investigation aimed to comprehensively

understand the magnetic fields, thermal radiation, and buoyancy forces in the presence of a porous surface. Senthilraja *et al.,* [31] conducted an experimental investigation into the energy analysis of a solar-powered hydrogen generation system using CuO/water nanofluids. Talukdar *et al.,* [32] described the incorporation of nanomaterials, such as MoS_2 and SiO_2, into base fluids has been shown to enhance the thermal conductivity and heat transfer capabilities of the resulting nanofluid. Moreover, the presence of velocity slip can significantly impact the flow characteristics and heat transfer performance, as it alters the velocity profile and boundary layer development. Jalili *et al.,* [33] concentrated on analyzing the complex dynamics of non-linear radiative heat transfer coupled with a magnetic field in a porous medium. The study specifically investigated how these factors influence the drift behavior of non-Newtonian Casson fluids. In a binary reactive Powell- Eyring fluid, Salawu *et al.,* [34] used a numerical scheme to assess the propagation of small particles and thermal radiation while accounting for the presence of thermophoresis, and Brownian motion. Azmi *et al.,* [35] investigated how the slip velocity presence at the boundary affects the unsteady MHD free convection flow of blood Casson fluid in a porous medium within a vertical cylinder. Yahaya *et al.,* [36] analyzed the flow of Al_2O_3-Cu/H_2O over a rotating disk with a uniform shrinking rate and injection. Reyaz *et al.,* [37] studied on fractional Caputo-Fabrizio Mxene Strontium Titanate hybrid nanofluid with Carboxymethyl Cellulose base flowing over a vertical uniform velocity Riga plate. Ullah *et al.,* [38] investigated the impact of gravity modulation, Joule heating and porous medium effects on magnetized nanofluid flow along radiative stretching sheet.

In many industrial and technical processes, the understanding of mass and heat transfer in chemical reactions is crucial. These processes are widely used in many industrial applications, including the food processing, ceramic or glassware manufacturing, and polymer production [39-43]. Manjunatha *et al.,* [44] looked at the importance of convective heat transfer and Stefan blowing in nanofluid flow across a curved stretching sheet with chemical reaction. Zeeshan *et al.,* [45] examined the energy analysis of non-Newtonian nanofluid flow over parabola of revolution on the horizontal surface with catalytic chemical reaction. Hussain *et al.,* [46] investigated the properties of dynamic wedges by exploring the chemically reacting flow through a heated porous wedge using the Powell-Eyring fluid model. Majeed *et al.,* [47] investigated the melting heat and mass transport characteristics on the stagnation point flow of Powell–Eyring nanofluid over a stretchable surface because melting is so important in many processes, such as Permafrost melting, magma solidification, and thawing of frozen grounds, are all examples of soil melting and freezing around the heat exchanger coils of a ground-based pump. Majeed *et al.,* [48] examined the influence of magnetized Casson nanofluid flow and heat transport phenomena towards a boundary layer flow over a nonlinear stretchable surface. Rehman *et al.,* [49] discussed the significance of nanoparticle diffusion and chemical reaction in the context of Powell-Eyring hybrid nanofluid flow over an expanding surface. The present research investigates the theoretical conclusions about the claims of anomalous heat transfer enhancement associated with nanofluids. The study by Shah *et al.,* [50] emphasized the crucial role of Ohmic dissipation and chemical reactions in the Powell-Eyring nanofluid flow across a stretching cylinder. Ullah *et al.,* [51] examined the heat and mass transportation of magneto nanofluid movement along a heated sheet with exponential temperature-dependent density, entropy optimization, thermal buoyancy, activation energy, and chemical reaction aspects. Ullah et al., [52] investigated the effects of activation energy and chemical reactions on the boundary layer flow around a wedge that is moving in a nanofluid. Ullah *et al.,* [53] studied the physical significance of heat generation and chemical reaction on Carreau nanofluid with convective heat conditions. Hussain et al., [54] analyzed the sensitivity of the movement of motile gyrotactic microorganisms to variation in Schmidt number, chemical reaction parameter, and Brownian motion parameter.

Considering the aforementioned discussion and practical uses of non-Newtonian nanofluid, it is noteworthy that no research has yet examined the Powell-Eyring nanofluid flow past a stretching surface when Stefan blowing or suction was present. The principal objective of this ongoing inquiry can be concisely stated as:

- To investigate the utilization of chemical reaction in the magnetized flow of Powell-Eyring nanofluid through an overextended sheet.
- The study delves into the thermal conduction of nanofluids, considering the impacts of thermal radiation alongside the characteristics of Brownian motion and thermophoresis parameter.
- The concentration equation undergoes modifications through the utilization of chemical reaction relations.
- The problem is represented by highly non-linear equations, and numerical simulations are effectively conducted using the bvp4c by MATLAB software.

2. Mathematical Formulation

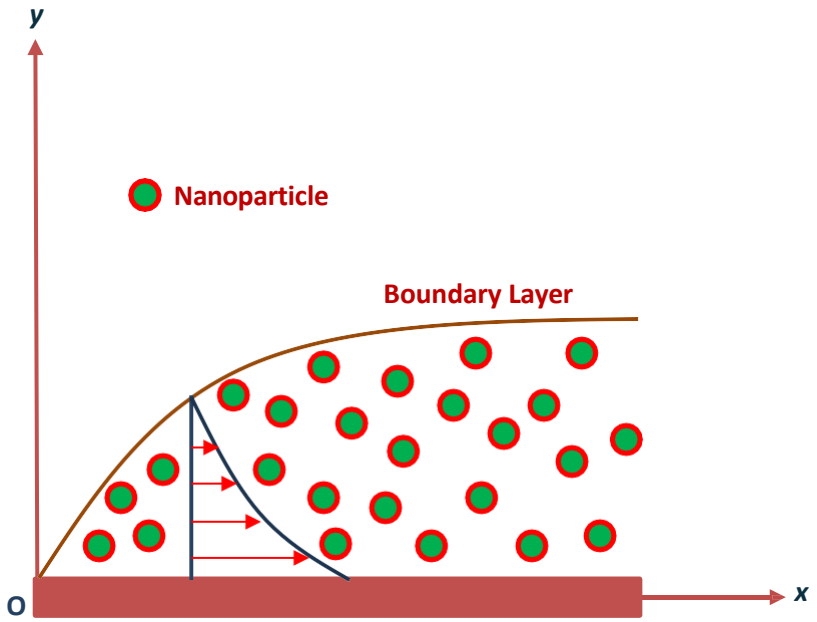


Fig. 1. Interpretation of flow geometry.

Consider the unsteady hydromagnetic flow of electrically conducting Powell-Eyring nanofluid over a stretching surface. On the surface, a magnetic field B_o is applied perpendicularly. The schematic diagram presented in Figure 1 depicts a complex network of interconnected elements, each playing a vital role in the overall functionality of the system. We may represent the dynamics of this system using a variety of techniques if we assume that a sheet starts stretching along the *x*-axis at time $t=0$ with velocity $U(x,t)=\frac{ax}{1-\alpha t}$ where the *y*-axis is perpendicular to the surface. We consider the impacts of Stefan blowing or suction and Lewis number. Brownian motion, chemical reactions, thermophoresis, and thermal radiations are closely intertwined phenomena that play a crucial role in various scientific and industrial applications. The Powell-Eyring nanofluid [13,19] rheological model is given by

$\tau = -pI + \tau_{ij}$, here I is identity vector, p is pressure, and the extra stress tensor

$$\tau_{ij} = \mu \frac{\partial u_i}{\partial x_j} + \frac{1}{\beta} \sinh^{-1}\left(\frac{1}{L}\frac{\partial u_i}{\partial x_j}\right),$$

in which $\sinh^{-1}\left(\frac{1}{L}\frac{\partial u_i}{\partial x_j}\right) \cong -\frac{1}{6L^3}\left(\frac{\partial u_i}{\partial x_j}\right)^3 + \frac{1}{L}\frac{\partial u_i}{\partial x_j}$ where $\left|\frac{\partial u_i}{\partial x_j}\right| << 1.$

The governing boundary layer equations under these presumptions can be written as [8,14,24]

$$\frac{\partial u}{\partial x} + \frac{\partial v}{\partial y} = 0 \tag{1}$$

$$\frac{\partial u}{\partial t} + u\frac{\partial u}{\partial x} + v\frac{\partial u}{\partial y} = \upsilon\left(1 + \frac{1}{\beta L \mu}\right)\frac{\partial^2 u}{\partial y^2} - \frac{1}{2\beta L^3 \rho}\left(\frac{\partial u}{\partial y}\right)^2 \frac{\partial^2 u}{\partial y^2} - \frac{\sigma B_o^2}{\rho} u \tag{2}$$

$$\frac{\partial T}{\partial t} + u\frac{\partial T}{\partial y} + v\frac{\partial T}{\partial y} = \frac{\kappa}{(\rho c_p)_f}\frac{\partial^2 T}{\partial y^2} + \frac{(\rho c_p)_p}{(\rho c_p)_f}\left[D_B \frac{\partial C}{\partial y}\frac{\partial T}{\partial y} + \frac{D_T}{T_\infty}\left(\frac{\partial T}{\partial y}\right)^2\right] + \frac{\mu}{(\rho c_p)_f}\left(1 + \frac{1}{\beta L \mu}\right)\left(\frac{\partial u}{\partial y}\right)^2 - \frac{1}{(\rho c_p)_f}\frac{\partial q_r}{\partial y} \tag{3}$$

$$\frac{\partial C}{\partial t} + u\frac{\partial C}{\partial x} + v\frac{\partial C}{\partial y} = D_B \frac{\partial^2 C}{\partial y^2} + \frac{D_T}{T_\infty}\frac{\partial^2 T}{\partial y^2} - k_r(t)(C - C_\infty) \tag{4}$$

The boundary conditions for the present analysis are [8,24]

$$\left.\begin{aligned} &u = U(x,t), v = -\frac{D_B}{1 - C_w}\frac{\partial C}{\partial y}, T = T_w, C = C_w \ \ at\ \ y = 0 \\ &u \to 0, T \to T_\infty, C \to C_\infty \ \ at\ \ y \to \infty \end{aligned}\right\} \tag{5}$$

Here the velocity components are denoted by *u* and *v*, respectively, in the *x*- and *y*-axis directions, $k_r(t) = k(1 - \alpha t)^{-1}$ is a chemical reaction parameter, k is constant, t denotes time, α is positive constant, $a > 0$ be any constant, μ is dynamic viscosity, υ is kinematic viscosity, β and L are fluid material constants, σ is electrical conductivity, $(\rho c_p)_f$ is heat capacity of the fluid, $(\rho c_p)_p$ is heat capacity of the nanoparticle material, κ is thermal conductivity, D_B is coefficient of Brownian diffusion, C is concentration, D_T is coefficient of thermophoresis diffusion, ρ is density of the fluid, $q_r = -\left(\frac{4\sigma}{3\chi}\right)\frac{\partial T^4}{\partial y}$ is radiative heat flux, σ^* is Stefan-Boltzmann constant, $T^4 \cong 4T_\infty^3 T - 3T_\infty^4$ (Higher order terms are neglected), T is temperature, T_w is surface temperature, C_w is surface nanoparticle

concentration, χ is Rosseland mean absorption coefficient, T_∞, C_∞ are the temperature and nanoparticle concentration distant from the exterior.

On simplifying Eq. (3), we get

$$\frac{\partial T}{\partial t}+u\frac{\partial T}{\partial x}+v\frac{\partial T}{\partial y}=\frac{\kappa}{(\rho c)_{pf}}\frac{\partial^2 T}{\partial y^2}+\frac{(\rho c)_p}{(\rho c)_{pf}}\left[D_B\frac{\partial C}{\partial y}\frac{\partial T}{\partial y}+\frac{D_T}{T_\infty}\left(\frac{\partial T}{\partial y}\right)^2\right]+\frac{\mu}{(\rho c)_{pf}}\left(1+\frac{1}{\beta L\mu}\right)\left(\frac{\partial u}{\partial y}\right)^2+\frac{1}{(\rho c)_{pf}}\frac{16\sigma^* T_\infty^3}{3\chi}\frac{\partial^2 T}{\partial y^2} \tag{6}$$

The skin friction coefficient $\left(C_f\right)$, and the rate of mass and heat transfer $\left(Sh_x, Nu_x\right)$can be described as

$$C_f=\frac{\tau_w}{\rho U^2},\ Nu_x=\frac{xq_w}{\kappa\left(T_w-T_\infty\right)},\ Sh_x=\frac{xq_m}{D_B\left(C_w-C_\infty\right)} \tag{7}$$

The surface mass and heat fluxes, shear stress near the wall are

$$q_m=-D_B\left(\frac{\partial C}{\partial y}\right)\Big|_{y=0},\ q_w=-\kappa\left(\frac{\partial T}{\partial y}\right)\Big|_{y=0},\ \tau_w=\left(\mu+\frac{1}{\beta L}\right)\left(\frac{\partial u}{\partial y}\right)\Big|_{y=0}-\frac{1}{6\beta L^3}\left(\frac{\partial u}{\partial y}\right)^3\Big|_{y=0}. \tag{8}$$

Now, we present the similarity variable η and the dimensionless functions g, θ, and ϕ as

$$\psi=x\sqrt{\frac{a\upsilon}{(1-\alpha t)}}g(\eta),\ \theta(\eta)=\frac{T-T_\infty}{T_\omega-T_\infty},\ \ \phi(\eta)=\frac{C-C_\infty}{C_\omega-C_\infty},\ \eta=y\sqrt{\frac{a}{\upsilon(1-\alpha t)}} \tag{9}$$

where ψ stands for stream function and is represented by the relationship that follows

$$u=\frac{\partial\psi}{\partial y}\quad v=-\frac{\partial\psi}{\partial x} \tag{10}$$

substituting Eqs. (9) and (10) into Eqs. (2), (6), and (4), we obtain the nonlinear ordinary differential equations:

$$\left[\left(1+k_0\right)-k_0\Lambda\left(g''\right)^2\right]g'''+g''g-A\left(g'+\frac{g''\eta}{2}\right)-\left(g'\right)^2-Mg'=0 \tag{11}$$

$$\frac{1}{Pr}\left(1+\frac{4}{3}R_d\right)\theta''+\left(1+k_0\right)Ec\left(g''\right)^2-\frac{A}{2}\eta\theta'+g\theta'+Nb\theta'\phi'+Nt\theta'^2=0 \tag{12}$$

$$\phi' - LePr\left[\left(\frac{A}{2}\eta - g\right)\phi' + \Gamma\phi\right] + \frac{Nt}{Nb}\theta' = 0 \tag{13}$$

The corresponding boundary conditions are

$$\left.\begin{aligned} g'(\eta) = 1,\ g(\eta) = \frac{S_0}{Le}\phi'(\eta),\ \theta(\eta) = 1,\ \phi(\eta) = 1 \ at \ \ \eta = 0 \\ g'(\eta) = 0,\ \theta(\eta) = 0,\ \phi(\eta) = 0 \ as \ \eta \to \infty \end{aligned}\right\} \tag{14}$$

Where $Le = \frac{\alpha_0}{D_B}$ (Lewis number) where $\alpha_0 = \frac{\kappa}{(\rho c_p)_f}$ (thermal diffusivity), $Nb = \frac{(\rho c_p)_p D_B (C_w - C_\infty)}{(\rho c_p)_f \upsilon}$ (Brownian motion), $Nt = \frac{(\rho c_p)_p D_T (T_w - T_\infty)}{(\rho c_p)_f T_\infty \upsilon}$ (thermophoresis parameter), $\Lambda = \left(ax/1-\alpha t\right)^3 / 2\nu x L^2$ (fluid parameter), $\Pr = \frac{\mu c_p}{\kappa}$ (Prandtl number), $k_0 = \frac{1}{\beta L \mu}$ (Eyring- Powell fluid parameter), $A = \frac{\alpha}{a}$ (unsteadiness parameter), $M = \frac{\sigma B^2 (1-\alpha t)}{\rho a}$ (magnetic field parameter), $R_d = \frac{4\sigma^* T^3}{\chi\kappa}$ (radiation parameter), $Ec = \left(ax/1-\alpha t\right)^2 / \left[c_p (T_w - T_\infty)\right]$ (Eckert number), $\Gamma = \frac{k}{a}$ (chemical reaction parameter), $S_0 = \frac{C_w - C_\infty}{1 - C_w}$ (Stefan blowing parameter) where $S_0 < 0$ and $S_0 > 0$ correspond to suction and blowing, respectively.

On simplifying Eq. (7), we get

$$C_f \mathrm{Re}_x^{0.5} = (1 + k_0)g''(0) - \frac{1}{3}k_0 \Lambda\left[g''(0)\right]^3, \ Nu_x \mathrm{Re}_x^{-0.5} = -\theta'(0), \ Sh_x \mathrm{Re}_x^{-0.5} = -\phi'(0) \tag{15}$$

where Reynolds number is denoted by $\mathrm{Re}_x = \frac{Ux}{\nu}$.

3. Solution Procedure

In our MATLAB computational approach, we utilize the bvp4c algorithm to solve dimensionless non-linear differential equations (11-13) alongside their corresponding boundary constraint (14). This involves employing the bvp4c solver within the MATLAB environment to derive numerical solutions for the ordinary differential equations. We first transform the dimensionless non-linear ODEs into a first-order initial boundary value problem to streamline this process. By using MATLAB's built-in bvp4c solver, we can achieve high accuracy in their numerical solutions. This is crucial for obtaining reliable results that reflect the physical phenomena being studied, such as the effects of thermal radiation, chemical reactions, and Stefan blowing on the flow of Eyring-Powell nanofluid. The numerical approach provides the flexibility to easily vary model parameters and

observe their effects on the system's behaviour. This capability is essential for understanding the sensitivity of the model and its applicability in various scenarios. The ensuing procedure delineates the necessary steps for obtaining the numerical solution.

$$g = h_1,\ g' = h_2,\ g'' = h_3,\ \theta = h_4,\ \theta' = h_5,\ \phi = h_6,\ \phi' = h_7 \tag{16}$$

$$h_3' = \frac{1}{\left[(1+k_0) - k_0\Lambda(h_3)\right]^2}\left[-h_3 h_1 + A\left(\frac{h_3\eta}{2} + h_2\right) + (h_2)^2 + M h_2\right] \tag{17}$$

$$h_5' = \frac{Pr}{\left(1+\frac{4}{3}R_d\right)}\left[-(1+k_0)Ec(h_3)^2 + \frac{A}{2}\eta h_5 - h_1 h_5 - Nb h_5 h_7 - Nt h_5^2\right] \tag{18}$$

$$h_7' = LePr\left[\left(\frac{A}{2}\eta - h_1\right)h_7 + \Gamma h_6\right] - \frac{Nt}{Nb}h_5' \tag{19}$$

Boundary conditions are

$$\left.\begin{aligned} &h_2 = 1,\ h_1 = \left(S_0 / Le\right)h_7,\ h_4 = 1,\ h_6 = 1 \quad at\ \eta = 0 \\ &h_2 = 0,\ h_4 = 0,\ h_6 = 0 \qquad\qquad at\ \eta = \infty \end{aligned}\right\} \tag{20}$$

4. Results and Discussions

Chemical reaction and radiation are taken into consideration while analyzing the Stefan blowing effect in an Eyring-Powell nanofluid via stretching sheet. Numerical techniques and similarity transformations are used to define and solve the governing equations. The findings are displayed in tables and graphs that show how important factors affect the profiles of temperature, velocity, and concentration. The influence of unsteady parameter A on the temperature, concentration and velocity fields is shown in Figure 2, Figure 3, and Figure 4. When discussing the temperature profile shown in the figures, explain how the unsteady parameter A influences heat transport. As A increases, the temperature profile rises significantly due to enhanced thermal energy accumulation, which can be attributed to the unsteady effects that improve heat transfer rates. Similarly, unsteadiness increases mass diffusion, which raises nanoparticle dispersion and causes concentration to rise dramatically. These impacts demonstrate how uneven flow alters the dynamics of heat and mass movement. Figure 5 illustrates when the velocity distribution partially decreases when the fluid parameter Λ increases. For the velocity distribution figure, it is important to describe how the fluid parameter Λ affects fluid resistance. Higher values of Λ lead to increased resistance, resulting in a decrease in overall flow velocity. This relationship can be explained by the non-Newtonian behaviour of the Eyring-Powell fluid, which becomes more pronounced as Λ increases. As the Eyring-Powell fluid parameter k_0 increases in Figure 6, and Figure 7, the non-Newtonian effects are lessened, which causes a progressive increase in velocity. At the same time, when k_0 rises, the temperature profile significantly drops, suggesting better thermal dissipation and less heat transfer resistance. The velocity field significantly decreases when the magnetic field parameter *M*

increases, as Figure 8 illustrates. This is due to fact that the retarding forces (called Lorentz forces) generated by the applied magnetic field act as resistive drag forces opposite to the flow direction, which results a decrease in velocity.

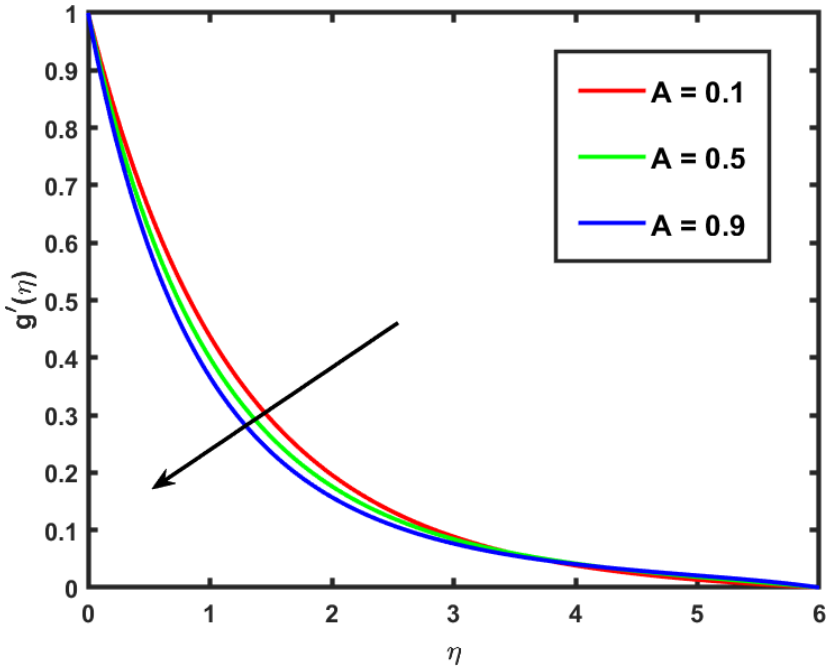


Fig. 2. Visual presentations of $g'(\eta)$ distribution with various A values.

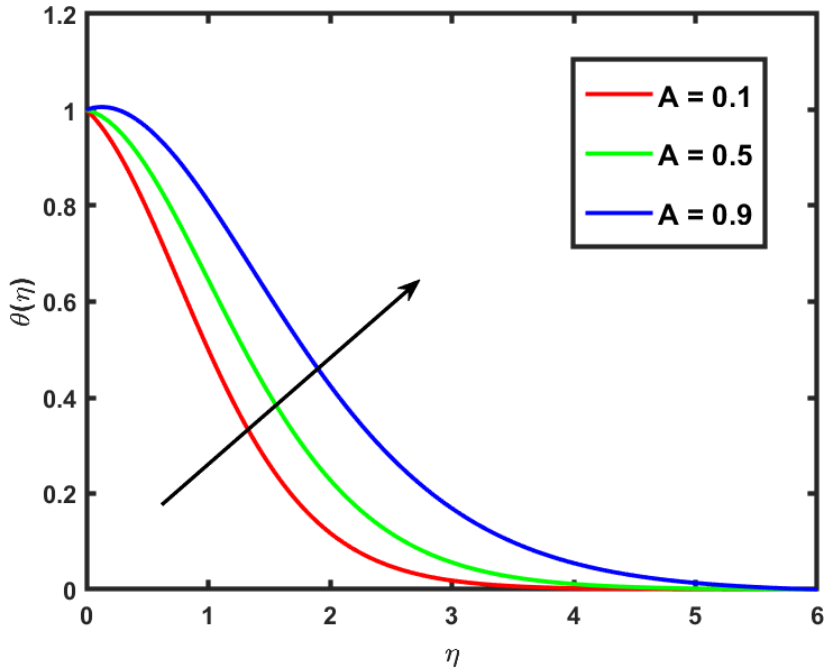


Fig. 3. Visual presentations of $\theta(\eta)$ distribution with various A values.

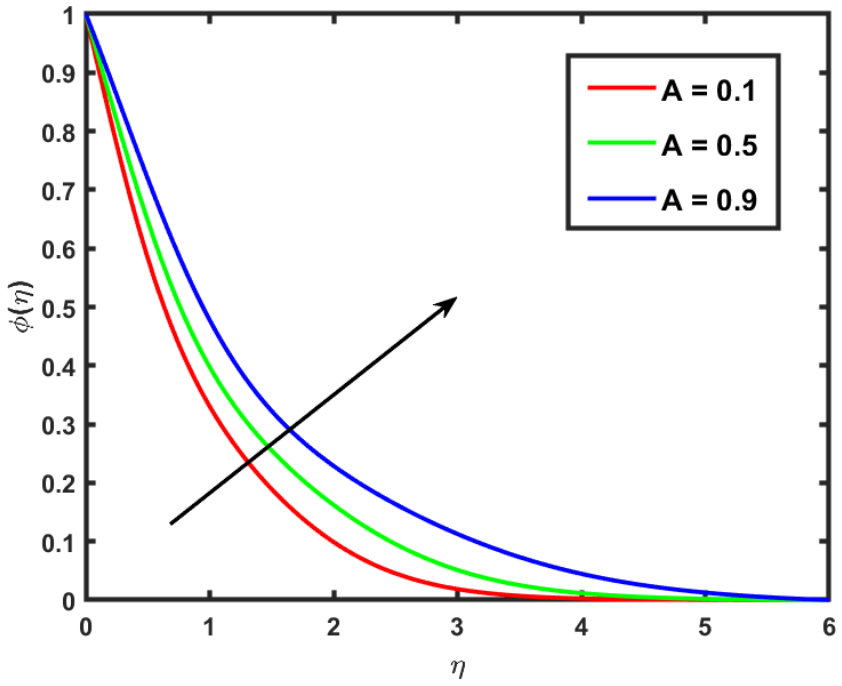


Fig. 4. Visual presentations of $\phi(\eta)$ distribution with various A values.

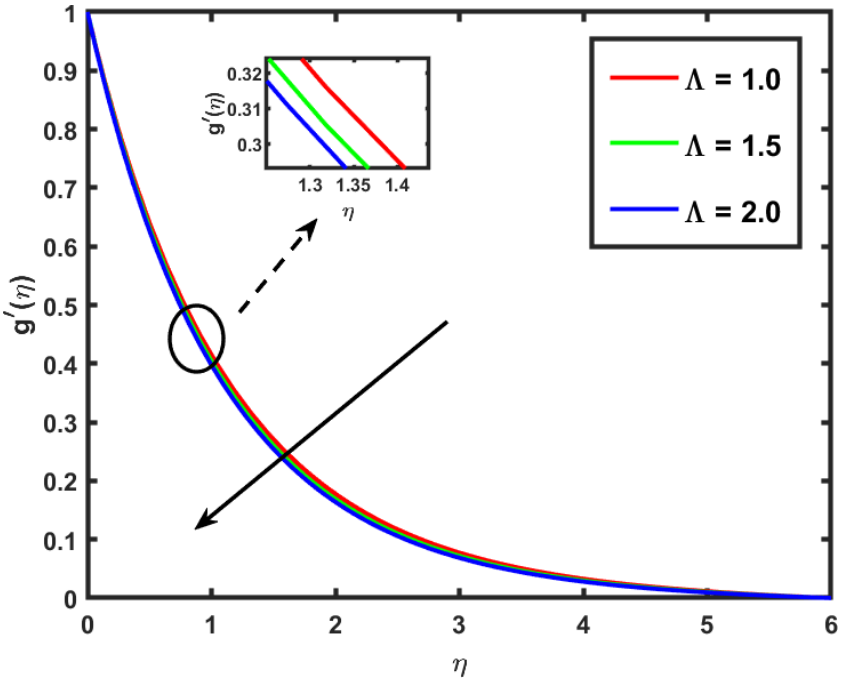


Fig. 5. Visual presentations of $g'(\eta)$ distribution with various Λ values.

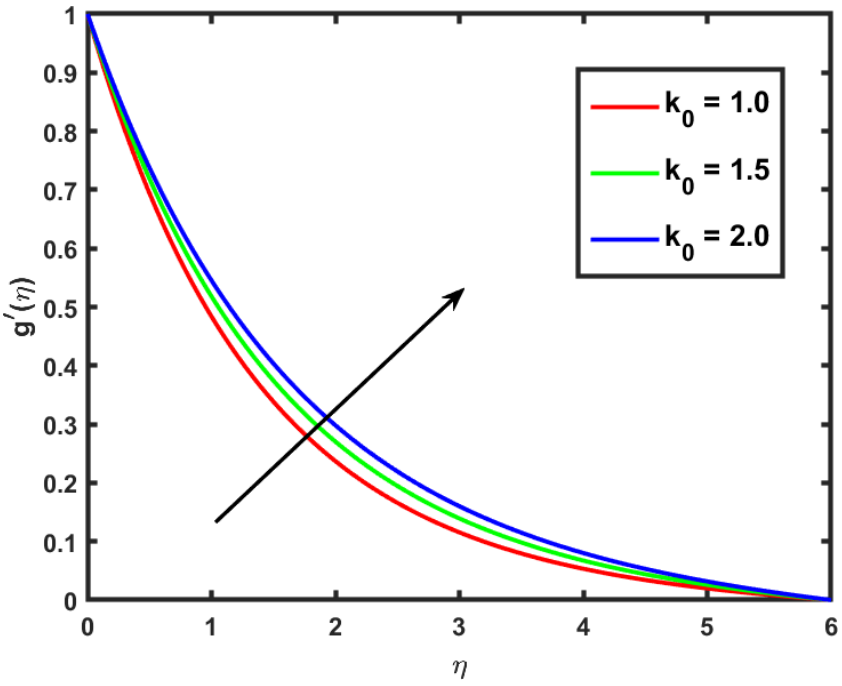


Fig. 6. Visual presentations of $g'(\eta)$ distribution with various k_0 values.

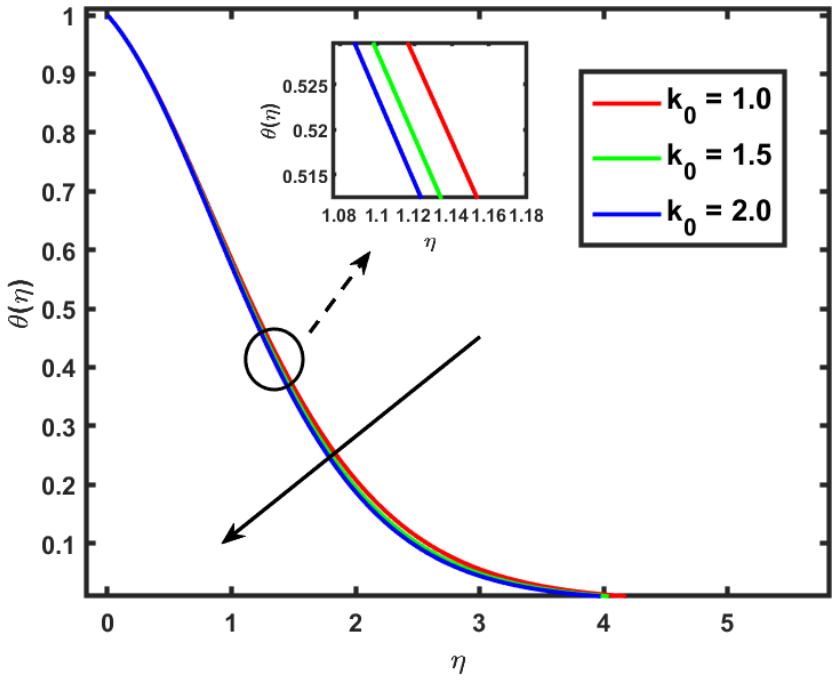


Fig. 7. Visual presentations of $\theta(\eta)$ distribution with various k_0 values.

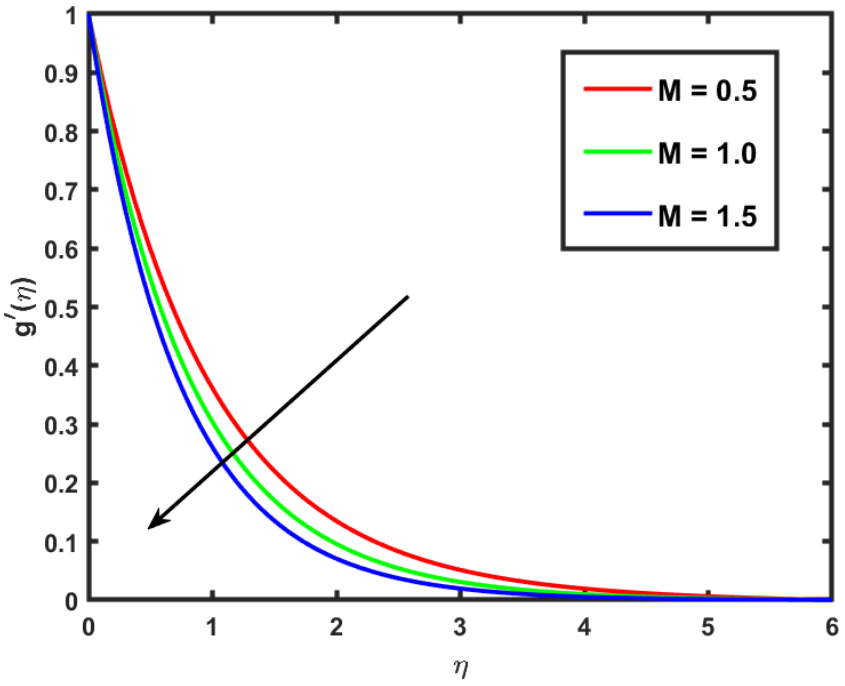


Fig. 8. Visual presentations of $g'(\eta)$ distribution with various M values.

Figure 9, Figure 10, and Figure 11 illustrate how a minor increase in the Stefan blowing parameter, S_0 raises the velocity while progressively raising the temperature and concentration. This happens because increased blowing effects propel fluid motion and marginally increase velocity by introducing more momentum into the boundary layer. A slow increase in temperature and concentration results from the improved mass transport close to the surface, which also lowers thermal and solutal boundary layer resistance. As seen in Figure 12, and Figure 13, the temperature progressively rises as the thermophoresis Nt and the Brownian motion parameter Nb increase. The random movement of nanoparticles is enhanced by Brownian motion, which accelerates thermal energy transfer and raises the temperature. By moving nanoparticles from hotter to cooler areas, thermophoresis also lowers heat dissipation and raises the temperature inside the boundary layer. As the Brownian motion strengthens, this leads to effective movement of nanoparticles from the walls to the fluid. Because of this reason, the dimensionless temperature θ increases with an increase in Nb. It may be noted that the parameters Nb and Nt characterize the strengths of Brownian motion and thermophoresis effects. The larger values of Nb and Nt, the larger the strength of the corresponding effects. Thus Nb and Nt can take any value in the range of $0 \le Nb;\ Nt < 1$. A rise in the radiation parameter as Figure 14 illustrates, R_d causes the temperature field to increase. For figure depicting the effects of thermal radiation, explain how increased radiation enhances the fluid's ability to absorb and release thermal energy, resulting in a higher temperature distribution. This relationship underscores the importance of thermal radiation in heat transfer processes. Figure 15 shows that a large drop in the concentration field occurs when the chemical reaction parameter Γ is increased. When addressing the concentration field, provide insights into how the chemical reaction parameter Γ impacts species concentration. An increase in Γ leads to a rapid consumption of species, resulting in a significant drop in concentration within the boundary layer. This can be explained by the faster reaction rates that deplete the available species. Figure 16 demonstrates that a large drop in the concentration field occurs when the Lewis number Le is increased.

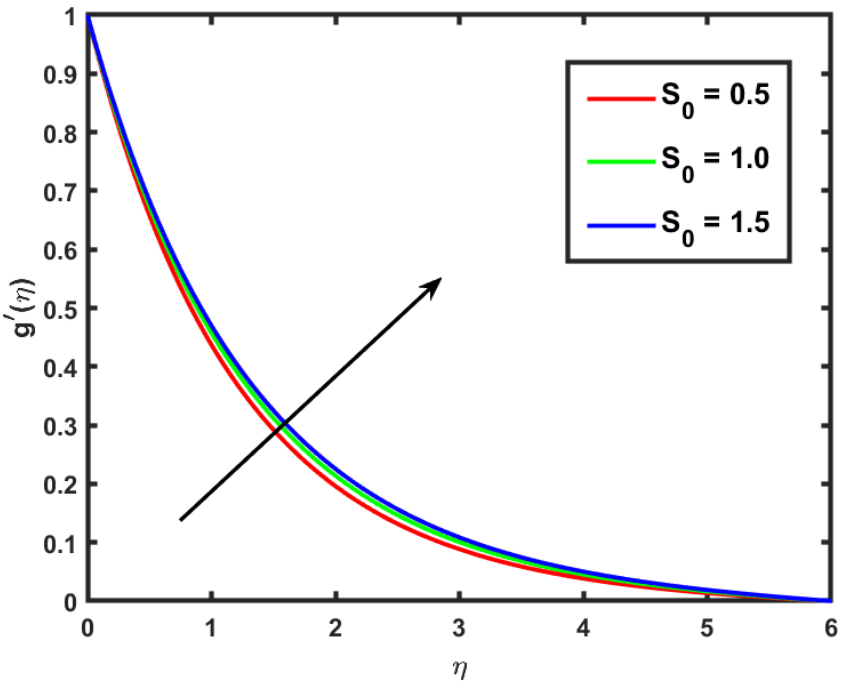


Fig. 9. Visual presentations of $g'(\eta)$ distribution with various S_0 values.

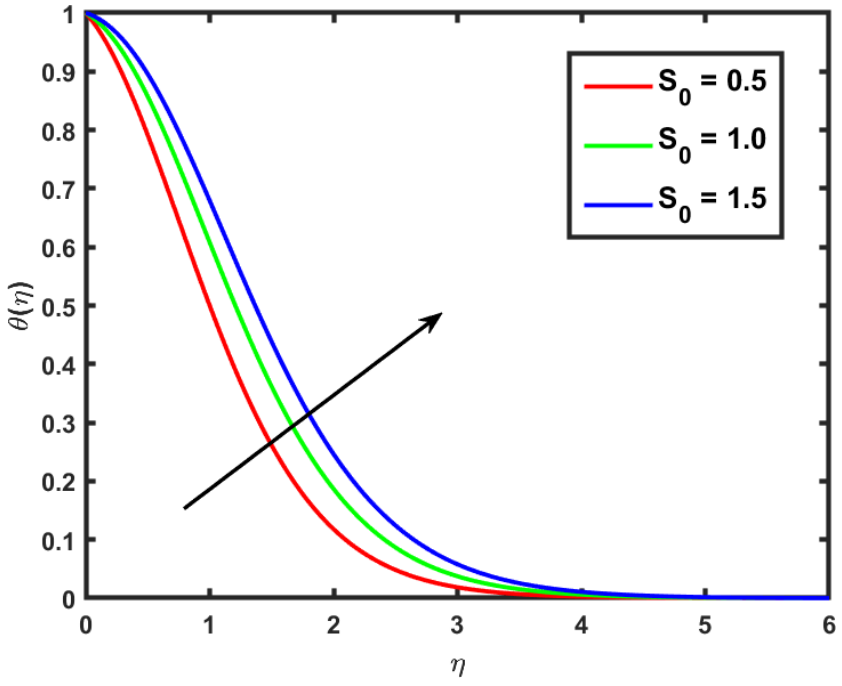


Fig. 10. Visual presentations of $\theta(\eta)$ distribution with various S_0 values.

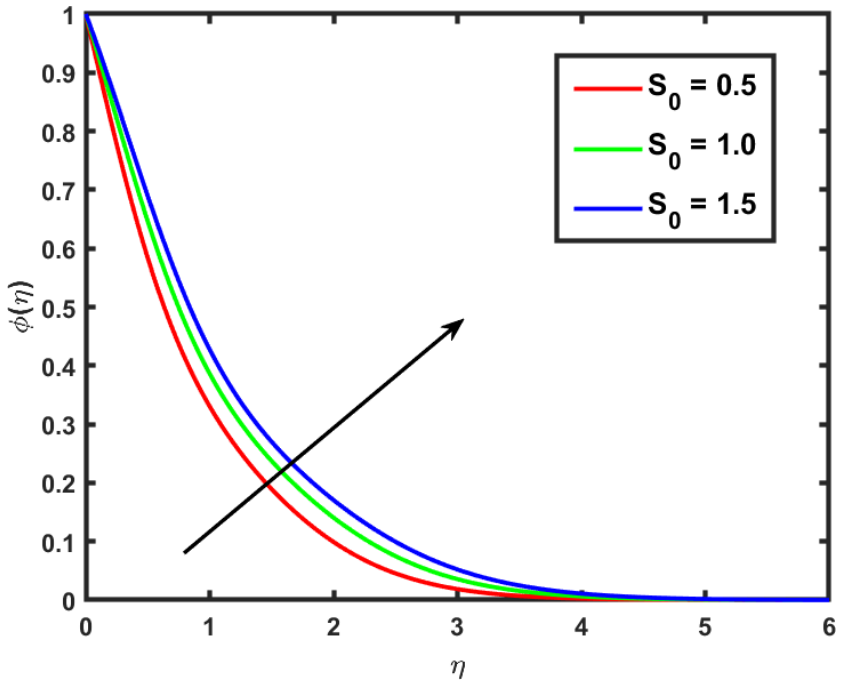


Fig. 11. Visual presentations of $\phi(\eta)$ distribution with various S_0 values.

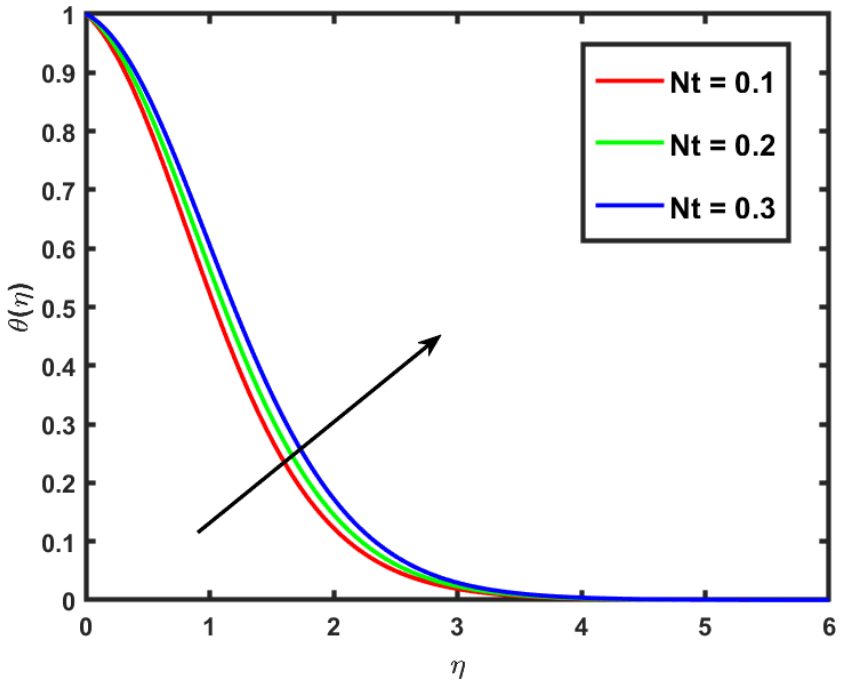


Fig. 12. Visual presentations of $\theta(\eta)$ distribution with various Nt values.

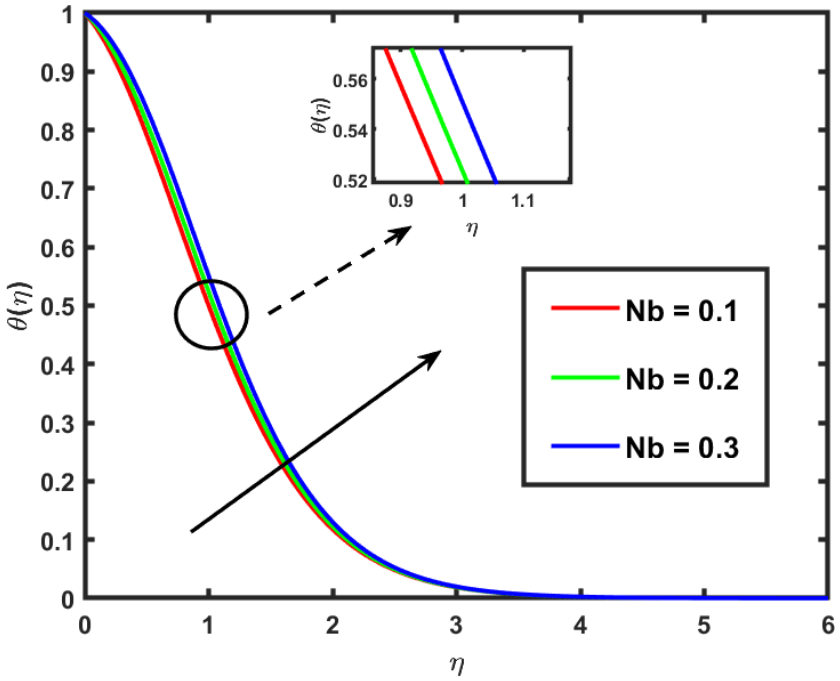


Fig. 13. Visual presentations of $\theta(\eta)$ distribution with various Nb values.

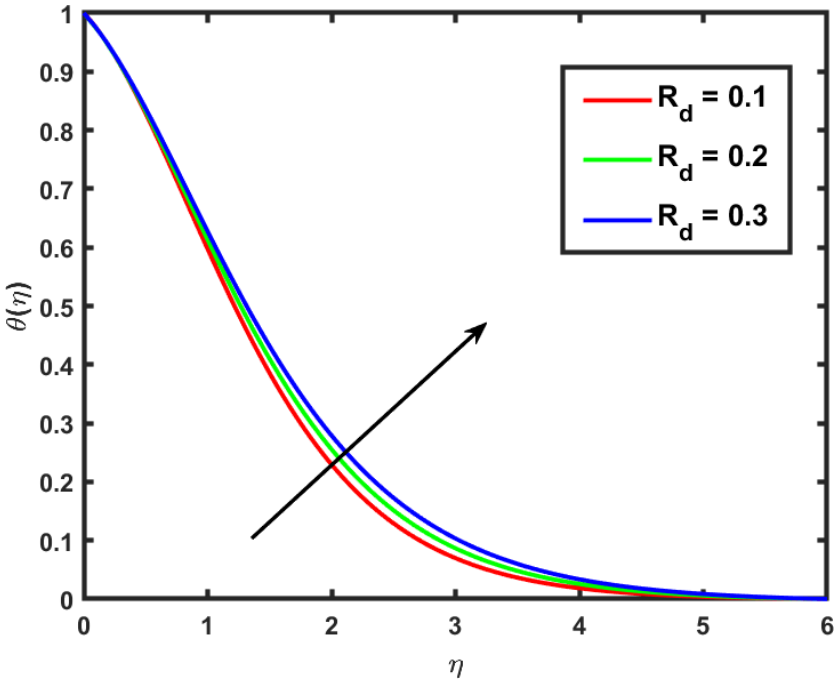


Fig. 14. Visual presentations of $\theta(\eta)$ distribution with various R_d values.

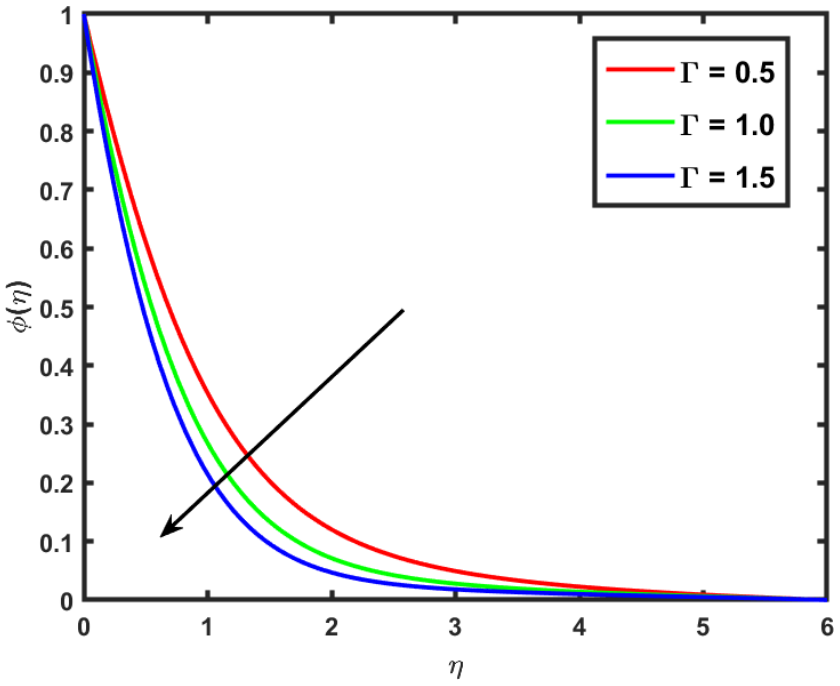


Fig. 15. Visual presentations of $\phi(\eta)$ distribution with various Γ values.

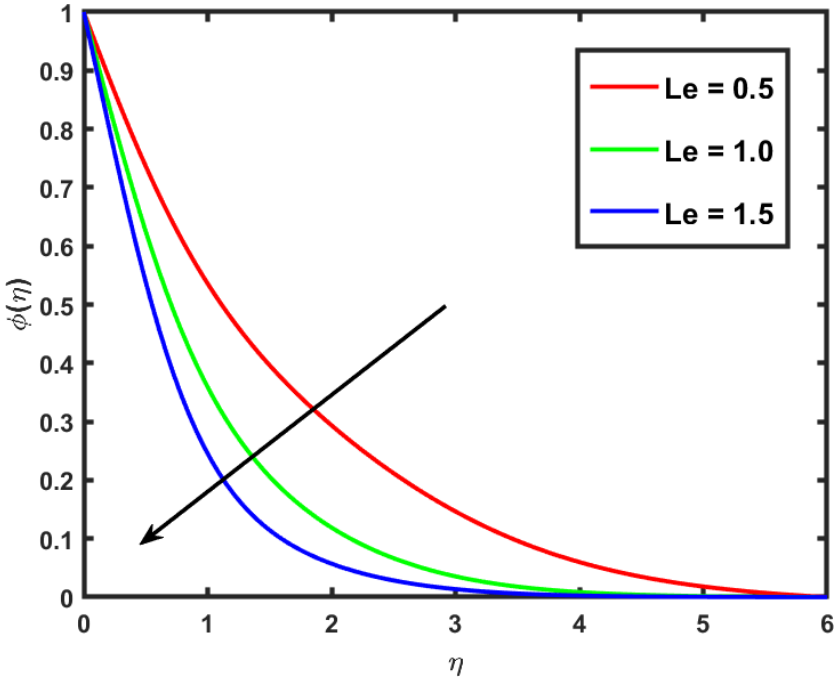


Fig. 16. Visual presentations of $\phi(\eta)$ distribution with various Le values.

The findings in Tables 1 and 2 demonstrate how important factors affect the gradients in temperature, concentration, and velocity. The falling temperature and concentration gradients show that increasing the Stefan blowing parameter S_0 promotes heat and mass transmission while

modestly increasing velocity. Likewise, the Powell–Eyring fluid parameter k_0 indicates a general improvement in thermal and solutal transport by strengthening the velocity gradient and slightly raising temperature and concentration levels. The flow is impacted by resistive forces, which may be caused by magnetic field effects, as indicated by the negative values of $C_f \mathrm{Re}_x^{0.5}$. Additionally, the comparison in Table 2 validates the computational technique by demonstrating great agreement between the current numerical results and earlier research.

Table 1
Represents the values of $C_f \mathrm{Re}_x^{0.5}$, $Nu_x \mathrm{Re}_x^{-0.5}$ and $Sh_x \mathrm{Re}_x^{-0.5}$ with $M = 0.2, \mathrm{Pr} = 21, Nb = 0.1, Le = 1.5, Nt = 0.1, R_d = 0.1, \Gamma = 0.5$ and $Ec = 0.1$

S_0	k_0	Λ	A	$C_f \mathrm{Re}_x^{0.5}$	$Nu_x \mathrm{Re}_x^{-0.5}$	$Sh_x \mathrm{Re}_x^{-0.5}$
0.1				-1.074137	-0.381340	-1.149444
0.3				-1.025079	-0.269335	-0.962300
0.5	0.1			-0.990639	-0.196971	-0.832775
	0.3			-0.920273	-0.196721	-0.845914
	0.5	0.1		-0.863036	-0.195706	-0.856717
		0.3		-0.970605	-0.061349	-0.712591
		0.5	0.1	-0.987402	-0.056825	-0.713197
			0.3	-0.919419	-0.143782	-0.808638
			0.5	-0.987402	-0.056825	-0.713197

Table 2
Numerical data of $C_f \mathrm{Re}_x^{0.5}$ for k_0, M, and Λ

k_0	M	Λ	Hayat *et al.,* [14]	Present values
0.0	0.1	0.1	-1.0832	-1.0839
0.1			-1.1324	-1.1321
0.2			-1.1802	-1.1799

5. Conclusions

This study delves into the behaviour of Eyring- Powell nanofluid flowing over an extending surface, examining the heat transference rate, and mass transference via physical experimentation and numerical simulations. The heat transfer rate also displays notable variability in response to alterations in the thermal radiation parameter. Numerical results are derived using the bvp4c by MATLAB software to solve the ordinary differential system, yielding significant insights, including:

- For greater (Λ), $g'(\eta)$ indicates a diminishing tendency, but for (k_0), the reverse trend is observed.
- Stefan blowing parameter (S_0) indicates a qualitative similarity between temperature and concentration profiles.

- Concentration $\phi(\eta)$ declines as Γ rises.
- Higher Lewis numbers Le indicate a dominance of thermal diffusivity over mass diffusivity, resulting in faster heat transfer but slower concentration adjustments. This finding underscores the importance of controlling the Lewis number Le to balance thermal and mass transfer in practical applications.
- The thermophoresis (Nt) and Brownian motion (Nb) parameters behave identically in the temperature field.
- Skin friction decreases for fluid parameter (Λ) and boosts up for the Stefan blowing parameter (S_0).

This work contributes novel insights into the interplay between thermal and mass transfer phenomena in non-Newtonian fluids, extending beyond previous studies by incorporating the effects of Stefan blowing and thermal radiation in a unified framework. The findings pave the way for future research into the application of Eyring-Powell nanofluids in advanced engineering systems, offering potential improvements in efficiency and performance across various sectors.

Future scope

The work can be modified by adding the impact of motile microorganisms, different nanoparticles, activation energy, and shaped change.

References

[1] Pantokratoras, A. "Study of MHD boundary layer flow over a heated stretching sheet with variable viscosity: A numerical reinvestigation." *International Journal of Heat and Mass Transfer* 51, no. 1-2 (2007): 104-110. https://doi.org/10.1016/j.ijheatmasstransfer.2007.04.007

[2] Kumar, Challa K. and Suripeddi Srinivas. "Influence of joule heating and thermal radiation on unsteady hydromagnetic flow of chemically reacting Casson fluid over an inclined porous stretching sheet." *Special Topics & Reviews in Porous Media an International Journal* 10, no. 4 (2019): 385-400. https://doi.org/10.1615/specialtopicsrevporousmedia.2019026908

[3] Hussain, Syed M., Mishra, Manas R., Seth, G. S., and Chamkha, Ali J. "Dynamics of heat absorbing and radiative hydromagnetic nanofluids through a stretching surface with chemical reaction and viscous dissipation." *Proceedings of the Institution of Mechanical Engineers Part E Journal of Process Mechanical Engineering* 238, no. 1 (2022): 101-111. https://doi.org/10.1177/09544089221096103

[4] Srinivas, S., Kumar, Challa K., Badeti, S., and Reddy, Anala S. (2023). MHD flow of casson nanofluid over an inclined porous stretching surface. *In Lecture notes in mechanical engineering*, Page 155-165. https://doi.org/10.1007/978-981-19-1929-9_13

[5] Anuar, Nur Syazana, Nur Adilah Liyana Aladdin, and Ioan Pop. "Darcy-Forchheimer flow of hybrid carbon nanotube over a permeable stretching shrinking curved surface." *Journal of Advanced Research in Fluid Mechanics and Thermal Sciences* 126, no. 2 (2025): 73-85. https://doi.org/10.37934/arfmts.126.2.7385

[6] Haider, Syed Muhammad A., Ali, B., Wang, Q., and Zhao, C. "Stefan blowing impacts on unsteady MHD flow of nanofluid over a stretching sheet with electric field, thermal radiation and activation energy." *Coatings* 11, no. 9 (2021): 1048. https://doi.org/10.3390/coatings11091048

[7] Abbas, W., Megahed, Ahmed M., Ibrahim, M. A., and Said, Ahmed A. M. "Ohmic dissipation impact on flow of Casson-Williamson fluid over a slippery surface through a porous medium." *Indian Journal of Physics* 97, no. 14 (2023): 4277-4283. https://doi.org/10.1007/s12648-023-02754-4

[8] Konai, S., Maiti, H., and Mukhopadhyay, S. "Influences of Stefan blowing on unsteady flow of Casson nanofluid past a stretching surface." *Forces in Mechanics* 12 (2023): 100227. https://doi.org/10.1016/j.finmec.2023.100227

[9] Sankari, M. S., Rao, M. E., Awwad, F. A., Ismail, Emad A. A., Makinde, O. D., and Khan, W. "Influence of dual stratification on the magnetohydrodynamic flow of Jeffrey nanofluid over an exponentially stretching permeable sheet with viscous dissipation and Joule heating." *Frontiers in Chemistry*, 12 (2025): 1451053. https://doi.org/10.3389/fchem.2024.1451053

[10] Zeb, H., Wahab, H. A., Khan, U., and Chamkha, A. J. "Magnetic dipole effects on non-Newtonian ferrofluid over a stretching sheet." *Heat Transfer* 52, no. 1 (2022): 759-779. https://doi.org/10.1002/htj.22715
[11] Ali, M. Y., Rahman, M., Ali, M. M., Ahmmed, S. F., and Haque, S. "Data analysis of non-linear radiative electro-periodic MHD flow past a stretching sheet with activation energy impact." *International Communications in Heat and Mass Transfer* 155 (2024): 107572. https://doi.org/10.1016/j.icheatmasstransfer.2024.107572
[12] Zhang, R., Zaydan, M., Alshehri, M., Raju, C., Wakif, A., and Shah, N. A. "Further insights into mixed convective boundary layer flows of internally heated Jeffery nanofluids: Stefan's blowing case study with convective heating and thermal radiation impressions." *Case Studies in Thermal Engineering* 55 (2024): 104121. https://doi.org/10.1016/j.csite.2024.104121
[13] Powell, Richard E. and Eyring, Henry. "Mechanisms for the relaxation Theory of viscosity." *Nature* 154 (1944): 427-428. https://doi.org/10.1038/154427a0
[14] Hayat, T., Sajjad, R., Muhammad, T., Alsaedi, A., and Ellahi, R. "On MHD nonlinear stretching flow of Powell–Eyring nanomaterial." *Results in Physics* 7 (2017): 535-543. https://doi.org/10.1016/j.rinp.2016.12.039
[15] Skadsem, Hans J., Leulseged, A., and Cayeux, E. "Measurement of drilling fluid rheology and modeling of thixotropic behavior." *Applied Rheology* 29, no. 1 (2019): 1-11. https://doi.org/10.1515/arh-2019-0001
[16] Srinivas, S., Challa, Kalyan K., Badeti, S., and Kumar, P. B. "Pulsatile Powell-Eyring nanofluid flow in a channel with inclined magnetic field and chemical reaction." *Engineering Transactions* 71, no. 4 (2023): 519-535. https://doi: 10.24423/EngTrans.2768.20231114
[17] Iskandar Waini, Anuar Ishak, and Ioan Pop. "Eyring-Powell Fluid Flow Past a Shrinking Sheet: Effect of Magnetohydrodynamic (MHD) and Joule Heating." *Journal of Advanced Research in Fluid Mechanics and Thermal Sciences* 116, no. 1 (2024): 64-77. https://doi.org/10.37934/arfmts.116.1.6477
[18] Khan, M. W. A., Khan, I., and Asif, M. "Applications of neural networking in Eyring-Powell nanofluid dynamics on a rotating surface in a porous medium." *Alexandria Engineering Journal* 108 (2024): 568-582. https://doi.org/10.1016/j.aej.2024.07.083
[19] Alsaedi, A., Hayat, T., Qayyum, S., and Yaqoob, R. "Eyring–Powell nanofluid flow with nonlinear mixed convection: Entropy generation minimization." *Computer Methods and Programs in Biomedicine* 186 (2019): 105183. https://doi.org/10.1016/j.cmpb.2019.105183
[20] Aljabali, A., Abdul Rahman Mohd Kasim, Najiyah Safwa Khashi'ie, Iskandar Waini, and Noor Amalina Nisa Ariffin. "Eyring-Powell Hybrid Nanofluid With Radiative Heat Flux: Case Over a Shrinking Sheet." *Journal of Advanced Research in Fluid Mechanics and Thermal Sciences* 111, no. 1 (2023): 109-121. https://doi.org/10.37934/arfmts.111.1.109121
[21] Allehiany, F., Riaz, A., Alfwzan, W. F., Shaheen, S., and Muhammad, T. "Cilia flow of magnetized Eyring-Powell nanofluid in a vertical thermal channel with viscous dissipation: An application of Adomian decomposition method." *Ain Shams Engineering Journal* 15, no. 5 (2024): 102699. https://doi.org/10.1016/j.asej.2024.102699
[22] Akinola, E., Salawu, S., Alao, S., and Oludoun, O. "Thermal distribution and viscous heating of electromagnetic radiative Eyring–Powell fluid with slippery wall conditions." *International Journal of Thermofluids* 24 (2024): 100841. https://doi.org/10.1016/j.ijft.2024.100841
[23] Ullah, Z., Alam, Md. M., El-Zahar, Essam. R., Abu-Zinadah, H., Seddek, Laila F., and Shahab, S. "Amplitude analysis of turbulent boundary layers and oscillatory heat transfer using Powell-Eyring nanofluid, exothermic reaction and periodic Stokes conditions." *Chaos, Solitons & Fractals* 193 (2025): 116155. https://doi.org/10.1016/j.chaos.2025.116155
[24] Challa, K. K., Rao, M. E., Jawad, M., Saidani, T., Abdallah, S. A. O., and Thenmozhi, D. "Enhanced heat transfer and flow dynamics of Powell-Eyring nanofluid: unsteady stretched surface and with Stefan blowing/suction." *Case Studies in Thermal Engineering* 65 (2025): 105664. https://doi.org/10.1016/j.csite.2024.105664
[25] Batool, K., Haq, F., Zainab, S., Anwar, S., Younis, J., Hussain, A., Alshammari, A. S., and El-Bahy, Z. M. "An investigation of heat transfer and optimization of entropy in bio-convective flow of Eyring-Powell nanomaterial with gyrotactic microorganisms." *Case Studies in Thermal Engineering* 61 (2024): 104903. https://doi.org/10.1016/j.csite.2024.104903
[26] Rikitu, Ebba H. and Makinde, Oluwole D. "Entropy generation and heat transfer analysis of Eyring-Powell nanofluid flow through inclined microchannel subjected to magnetohydrodynamics and heat generation." *International Journal of Thermofluids* 22 (2024): 100640. https://doi.org/10.1016/j.ijft.2024.100640
[27] Tabrez, M., Khan, Waqar A., Hussain, I., Ali, M., and Muhammad, T. "Significance of radiative heat transfer analysis for magnetized Eyring Powell fluid comprising moment of tiny ferromagnetic nanoparticles and viscous dissipation." *Journal of Radiation Research and Applied Sciences* 18, no. 1 (2024): 101219. https://doi.org/10.1016/j.jrras.2024.101219

[28] Bhaskar, K., Sharma, K., and Bhaskar, K. "Exploring the gyrotactic microorganisms flow over cylinder/plate with Eyring-Powell model and hybrid nanofluids of varied nanoparticle shapes." *International Journal of Thermofluids* 26 (2025): 101068. https://doi.org/10.1016/j.ijft.2025.101068
[29] Daniel, Yahaya S. and Daniel, Simon K. "Effects of buoyancy and thermal radiation on MHD flow over a stretching porous sheet using homotopy analysis method." *Alexandria Engineering Journal* 54, no. 3 (2015): 705-712. https://doi.org/10.1016/j.aej.2015.03.029
[30] Chamkha, Ali J. "Thermal radiation and buoyancy effects on hydromagnetic flow over an accelerating permeable surface with heat source or sink." *International Journal of Engineering Science* 38, no. 15 (2000): 1699-1712. https://doi.org/10.1016/s0020-7225(99)00134-2
[31] Senthilraja, S., Gangadevi, R., Köten, H., Thangavel, S., Baskaran, M., and Awad, Mohamed M. "Energy analysis of solar powered hydrogen production system with CuO/water nanofluids: An experimental investigation." *Journal of King Saud University - Engineering Sciences* 35, no. 8 (2023): 525-530. https://doi.org/10.1016/j.jksues.2023.09.001
[32] Talukdar, B., Pal, D., and Vajravelu, K. "Analysis of Magnetohydrodynamic Oscillatory Convective Radiative Heat Flow of Reactive Nanofluid Containing MoS2 and SiO2 Nanoparticles with Velocity Slip." *Journal of Nanofluids* 12, no. 8 (2023): 2026-2043. https://doi.org/10.1166/jon.2023.2061
[33] Jalili, P., Azar, Ali A., Jalili, B., and Ganji, Davood D. "Study of nonlinear radiative heat transfer with magnetic field for non-Newtonian Casson fluid flow in a porous medium." *Results in Physics* 48 (2023): 106371. https://doi.org/10.1016/j.rinp.2023.106371
[34] Salawu, S. O., Yusuf, T. A., Obalalu, A. M., and Fatunmbi, E. O. "Thermal radiation and propagation of tiny particles in magnetized Eyring–Powell binary reactive fluid with generalized Arrhenius kinetics." *Case Studies in Thermal Engineering* 58 (2024): 104409. https://doi.org/10.1016/j.csite.2024.104409
[35] Azmi, W. F. W., Mohamad, Ahmad Q., Jiann, Lim Y., and Shafie, S. "Porosity and slip velocity effects on MHD pulsatile Casson fluid in a cylinder." *Semarak International Journal of Nanotechnology* 1, no. 1 (2024): 13-28.
[36] Yahaya, Rusya I., Arifin, Norihan M., Pop, I., Ali, Fadzilah M., and Isa, S. S. P. M. "Flow and heat transfer analysis of hybrid nanofluid over a rotating disk with a uniform shrinking rate in the radial direction: Dual solutions." *Semarak International Journal of Nanotechnology* 1, no. 1 (2024): 29-44.
[37] Reyaz, R., Mohamad, Ahmad Q., Lim, Yeou J., Khan, A., and Shafie, S. "Mxene and strontium titanate hybrid Casson nanofluid with CMC base via the Caputo-Fabrizio fractional derivative over a vertical Riga plate." *Semarak International Journal of Nanotechnology* 1, no. 1 (2024): 45-64.
[38] Ullah, Z., El-Zahar, Essam. R., Seddek, Laila F., Eladeb, A., Kolsi, L., Alsharari, Abdulrhman M., Asad, J., and Akgül, A. "Microgravity analysis of periodic oscillations of heat and mass transfer of Darcy-Forchheimer nanofluid along radiating stretching surface with Joule heating effects." *Results in Physics* 62 (2024): 107810. https://doi.org/10.1016/j.rinp.2024.107810
[39] Rao, M. E. and Sreenadh, S. "MHD flow of a Casson fluid over an exponentially inclined permeable stretching surface with thermal radiation, viscous dissipation and chemical reaction." *Global Journal of Pure and Applied Mathematics* 13, no. 10 (2017): 7529-7548.
[40] Srinivas, S., Kumar, Challa K., and Reddy, Anala S. "Pulsating flow of Casson fluid in a porous channel with thermal radiation, chemical reaction and applied magnetic field." *Nonlinear Analysis Modelling and Control* 23, no. 2 (2018): 213-233. https://doi.org/10.15388/na.2018.2.5
[41] Nadeem, M., Siddique, I., Din, I. S. U., Awwad, F. A., Ismail, E. A. A., and Ahmad, H. "Impact of chemical reaction on Eyring–Powell fluid flow over a thin needle with nonlinear thermal radiation." *Scientific Reports* 13, no. 1 (2023): 21401. https://doi.org/10.1038/s41598-023-48400-1
[42] Thenmozhi, D., Rao, M. E., Devi, R. R., Nagalakshmi, C., and Selvi, P. "Dynamics of heat transfer in complex fluid systems: comparative analysis of Jeffrey, Williamson and Maxwell fluids with chemical reactions and mixed convection." *International Journal of Thermofluids* 24 (2024): 100896. https://doi.org/10.1016/j.ijft.2024.100896
[43] Khan, M. I., Zeeshan, A., Ellahi, R., and Bhatti, M. M. "Advanced Computational Framework to Analyze the Stability of Non-Newtonian Fluid Flow through a Wedge with Non-Linear Thermal Radiation and Chemical Reactions." *Mathematics* 12 (2024): 1420. https://doi.org/10.3390/math12101420
[44] Manjunatha, P. T., Chamkha, A. J., Gowda, R. J. P., Kumar, R. N., Prasannakumara, B. C., and Naik, S. M. "Significance of Stefan blowing and convective heat transfer in nanofluid flow over a curved stretching sheet with chemical reaction." *Journal of Nanofluids* 10, no. 2 (2021): 285-291. https://doi.org/10.1166/jon.2021.1786
[45] Zeeshan, A., Awais, M., Alzahrani, F., Shehzad, N. "Energy analysis of non-Newtonian nanofluid flow over parabola of revolution on the horizontal surface with catalytic chemical reaction." *Heat Transfer* 50, no. 6 (2021): 6189-6209. https://doi.org/10.1002/htj.22168
[46] Hussain, M., Ranjha, Q. A., Anwar, M. S., Jahan, S., and Ali, A. "Eyring-Powell model flow near a convectively heated porous wedge with chemical reaction effects." *Journal of the Taiwan Institute of Chemical Engineers* 139 (2022): 104510. https://doi.org/10.1016/j.jtice.2022.104510

[47] Majeed, A., Zeeshan, A., Jawad, M., and Alhodaly, M. Sh. "Influence of melting heat transfer and chemical reaction on the flow of non-Newtonian nanofluid with Brownian motion: Advancement in mechanical engineering." *Proceedings of the Institution of Mechanical Engineers, Part E* 238, no. 1 (2022):396-404. https://doi:10.1177/09544089221145527

[48] Majeed, A., Rifaqat, S., Zeeshan, A., Alhodaly, M. Sh., and Noori, F. M. "Impact of velocity slip and radiative magnetized Casson nanofluid with chemical reaction towards a nonlinear stretching sheet: Three-stage Lobatto collocation scheme." *International Journal of Modern Physics B* 37, no. 9 (2023): 2350088. https://doi.org/10.1142/S0217979223500881

[49] Rehman, S., Hashim, N., Alqahtani, S., Alshehery, S., and Boujelbene, M. "Modelling heat-mass transport for MHD Eyring-Powell hybrid nanofluid over an expanding surface laden by autocatalytic chemical reaction and nanoparticles diffusion." *Advances in Engineering Software* 186 (2023): 103549. https://doi.org/10.1016/j.advengsoft.2023.103549

[50] Shah, Z., Waqas, M., Raja, M. a. Z., Shahzad, F., Zamri, N., Juraev, N., and Alanazi, M. M. "Dynamics of stratified-convected Eyring-Powell nanoliquid featuring chemically reactive species and Ohmic dissipation: Application of Levenberg-Marquardt artificial neural networks(ALM-ANNs)." *International Journal of Heat and Fluid Flow* 108 (2024): 109464. https://doi.org/10.1016/j.ijheatfluidflow.2024.109464

[51] Ullah, Z., Alam, Md. Mahbub., Khan, Aamir A., Alkarni, S., Merga, Feyisa E., and Khan, Q. "Analysis of activation energy, chemical reaction, and variable density on magnetically driven heat transportation: Applications in nanofluid lubrication and machining." *AIP Advances* 14, no. 10 (2024): 105020. https://doi.org/10.1063/5.0231088

[52] Ullah, Z., Alam, Md. Mahbub., Khan, Aamir A., Malik, A., Alkarni, S., Khan, Q., and Merga, Feyisa E. "Thermally and chemically reactive boundary layer flow past a wedge moving in a nanofluid with activation energy and thermophoretic diffusion effects." *AIP Advances* 14, no. 10 (2024): 105225. https://doi.org/10.1063/5.0235052

[53] Ullah, Z., Alam, Md. Mahbub., Tariq, U., Mahrous, Y. M., Merga, Feyisa E., Albouchi, F., Haider, I., Faqihi, and Abdullah A. "Variable density and heat generation impact on chemically reactive carreau nanofluid heat-mass transfer over stretching sheet with convective heat condition." *Case Studies in Thermal Engineering* 63 (2024): 105260. https://doi.org/10.1016/j.csite.2024.105260

[54] Hussain, D., Asghar, Z., Zeeshan, A., and Masud, U. "Sensitivity evaluation of Brownian motion and chemical reaction parameter on transport of motile gyrotactic microorganism in nanofluid over a wedge." *Journal of Applied Mathematics and Mechanics* 105, no. 2 (2025): e202200528. https://doi.org/10.1002/zamm.202200528